THE JOURNAL OF BIOLOGICAL CHEMISTRY VOL. 288, NO. 2, pp. 1200–1213, January 11, 2013

Biphasic Regulation of Myosin Light Chain Phosphorylation by p21-activated Kinase Modulates Intestinal Smooth Muscle Contractility*[S]

Received for publication, April 10, 2012, and in revised form, November 2, 2012 Published, JBC Papers in Press, November 16, 2012, DOI 10.1074/jbc.M112.370718

Ji Chu[‡], Ngoc T. Pham[‡], Nicole Olate[‡], Karina Kislitsyna[‡], Mary-Clare Day[‡], Phillip A. LeTourneau[‡], Alexander Kots[§], Randolph H. Stewart[¶], Glen A. Laine[¶], Charles S. Cox, Jr.[‡¶], and Karen Uray[‡¶1]

From the [‡]Department of Pediatric Surgery, University of Texas Medical School, Houston, Texas 77030, the [§]Department of Biochemistry and Molecular Biology, School of Medicine and Health, George Washington University, Washington, D. C. 20037, and the [¶]Michael E. DeBakey Institute, Texas A&M University, College Station, Texas 77483

Background: Myosin light chain (MLC) phosphorylation is the driving force of cell contractility.
Results: p21-activated kinase (PAK) can either activate or inhibit myosin light chain phosphorylation, depending on the level of PAK activation.
Conclusion: Inhibition of intestinal motility by supraphysiological mechanical stretch is attributable to increased PAK activity.
Significance: The biphasic regulation of PAK may provide an explanation for the conflicting observations on PAK-mediated MLC phosphorylation.

Supraphysiological mechanical stretching in smooth muscle results in decreased contractile activity. However, the mechanism is unclear. Previous studies indicated that intestinal motility dysfunction after edema development is associated with increased smooth muscle stress and decreased myosin light chain (MLC) phosphorylation *in vivo*, providing an ideal model for studying mechanical stress-mediated decrease in smooth muscle contraction. Primary human intestinal smooth muscle cells (hISMCs) were subjected to either control cyclical stretch (CCS) or edema (increasing) cyclical stretch (ECS), mimicking the biophysical forces in non-edematous and edematous intestinal smooth muscle *in vivo*. ECS induced significant decreases in phosphorylation of MLC and MLC phosphatase targeting subunit (MYPT1) and a significant increase in p21-activated kinase (PAK) activity compared with CCS. PAK regulated MLC phosphorylation in an activity-dependent biphasic manner. PAK activation increased MLC and MYPT1 phosphorylation in CCS but decreased MLC and MYPT1 phosphorylation in hISMCs subjected to ECS. PAK inhibition had the opposite results. siRNA studies showed that PAK1 plays a critical role in regulating MLC phosphorylation in hISMCs. PAK1 enhanced MLC phosphorylation via phosphorylating MYPT1 on Thr-696, whereas PAK1 inhibited MLC phosphorylation via decreasing MYPT1 on both Thr-696 and Thr-853. Importantly, *in vivo* data indicated that PAK activity increased in edematous tissue, and inhibition of PAK in edematous intestine improved intestinal motility. We conclude that PAK1 positively regulates MLC phosphorylation in intestinal smooth muscle through increasing inhibitory phosphorylation of MYPT1 under physiologic conditions, whereas PAK1 negatively regulates MLC phosphorylation via inhibiting MYPT1 phosphorylation when PAK activity is increased under pathologic conditions.

As a primary site for food digestion and transduction, intestinal smooth muscle is constantly receiving external pressure and mechanical stress. Therefore, the response of the intestinal smooth muscle to mechanical stimulation is among the most important adaption responses to the outside environment. Increased contraction in response to mechanical stretch of smooth muscle is a common response observed in multiple systems, including the intestine (1–5), which is important in maintaining normal organ function. However, persistent or supraphysiological stretch has been shown to decrease smooth muscle cell contraction and may trigger dysfunction leading to severe clinical consequences (5–7). The mechanism of stretch-mediated decrease of smooth muscle contraction is unclear.

Intestinal edema development is one instance when intestinal smooth muscle cells are subjected to persistently increased stretch. Intestinal edema develops under various pathologic conditions, such as trauma with fluid resuscitation, abdominal surgery, heart failure, or traumatic brain injury (8–10). Intestinal edema causes a 6-fold increase in strain in the smooth muscle layer of the intestine compared with non-edematous tissue (11). This increased strain, resulting in increased stretching force to the intestinal smooth muscle cells, is associated with decreased intestinal contractile activity via decreased myosin light chain (MLC)[2] phosphorylation (12–15). This is accomplished by edema-induced attenuation of the constitutive inhibition of MLC phosphatase in intestinal smooth muscle (7). The mechanism by which intestinal mechanical stress alters the

* This work was supported, in whole or in part, by National Institutes of Health, NIDDK, Grants KO1 DK 070758 and P30 DK56338.
[S] This article contains supplemental Figs. S1–S4.
[1] To whom correspondence should be addressed: Dept. of Pediatric Surgery, University of Texas Medical School, Houston, TX 77030. Tel.: 713-500-6196; Fax: 713-500-7296; E-mail: karen.l.davis@uth.tmc.edu.

[2] The abbreviations used are: MLC, myosin light chain; MLCK, MLC kinase; BPIPP, 5-(3-bromophenyl)-5,11-dihydro-1,3-dimethyl-1*H*-indeno[2′,1′:5,6]pyrido[2,3-*d*]pyrimidine-2,4,6(3*H*)-trione; ROCK, Rho kinase; PAK, p21-activated kinase; hISMC, human intestinal smooth muscle cell; CCS, control cyclical stretch; ECS, edema cyclical stretch; ca-PAK1, constitutively active PAK1; kn-PAK1, kinase-negative PAK1.

regulation of MLC phosphorylation is poorly understood. Understanding the response of intestinal smooth muscle cells to stretch will help in understanding the mechanotransduction pathway in regulating MLC phosphorylation; it will also aid in identifying therapeutic targets for treating edema-induced motility disorders.

Thr-18 and Ser-19 are two common phosphorylation sites of MLC. The interaction between myosin and actin, regulated by MLC phosphorylation especially at Ser-19, is the driving force for smooth muscle cell contraction (16, 17). MLC phosphorylation is precisely regulated by Ca^{2+}/calmodulin-dependent MLC kinase (MLCK) and MLC phosphatase (18–20). MYPT1, the myosin binding subunit of MLC phosphatase, is regulated via phosphorylation of two sites, threonine 696 (Thr-696) and threonine 853 (Thr-853) (21). Phosphorylation of these two sites inhibits MLC phosphatase activity. Numerous kinases have been reported to phosphorylate MYPT1, including Rho kinase (ROCK), zipper-interacting protein kinase, integrin-linked kinase, and p21-activated kinase (PAK) (22–24).

PAKs, are a group of Rac- and Cdc42-regulated serine/threonine protein kinases participating in many mechanotransduction pathways and involved in multiple biologic processes, including cytoskeletal dynamics, cell motility, angiogenesis, and cancer metastasis (25–27). There are two subgroups of PAK, group I PAK (PAK1 to -3) and group II (PAK4 to -6). Group I PAK activity is critical to cytoskeletal organization, cell motility, movement, and migration, which all involve MLC phosphorylation. The regulatory role of PAK in MLC phosphorylation has been reported in several studies (28–31). However, the results are controversial. PAK has been shown to increase MLC phosphorylation and cell motility through enhanced inhibitory MYPT1 phosphorylation or by directly phosphorylating MLC (22, 28, 30). In contrast, PAK has been shown to inhibit MLC phosphorylation by phosphorylating and inhibiting MLCK (32).

In the current studies, the role of PAK in the mechanotransductive regulation of MLC phosphorylation and intestinal smooth muscle contraction has been investigated. These findings will help us to further understand PAK-regulated MLC phosphorylation, identify new drug targets, and design better therapeutic methods to treat motility disorders. It may also help us to understand the regulation of smooth muscle contraction in response to mechanical stimuli.

EXPERIMENTAL PROCEDURES

Human Primary Cell Isolation and Culture—Disease-free small intestinal tissue was collected from organ donor patients with the generous consent of a family member and approval by the Committee for the Protection of Human Subjects at University of Texas Health Science Center at Houston. The human ileal muscularis externa was separated from mucosal and submucosal tissue, cut into small pieces, and incubated in Ca^{2+}-free Hanks' balanced salt solution (pH 7.4) (Cellgro®, Manassas, VA) (37 °C, 15 min), followed by incubation in Ca^{2+}-free Hanks' balanced salt solution containing 0.38 mg/ml papain and 15 ng/ml DTT until tissue became loose and sticky. After washing with HEPES buffer (120 mM NaCl, 4 mM KCl, 2.6 mM KH_2PO_4, 2 mM $CaCl_2$, 0.6 mM $MgCl_2$, 25 mM HEPES, 14 mM glucose, 2.1% essential amino acid mixture), muscle tissue was digested with 0.21 mg/ml collagenase type II (Worthington) and 0.1 mg/ml soybean trypsin inhibitor (30 min, 31 °C) (Worthington). After washing with HEPES buffer again, human intestinal smooth muscle cells (hISMCs) were harvested by filtration through 500-μm Nitex mesh and cultured in Smooth Muscle Cell Growth Medium 2 with 5% fetal calf serum (PromoCell®, Heidelberg, Germany), 100 units/ml penicillin, 100 μg/ml streptomycin, and 0.25 μg/ml amphotericin B in a 5% CO_2 incubator. To avoid dedifferentiating cells, only passage 1–3 hISMCs were used in the current studies.

Cell Stretching—hISMCs were seeded onto 6-well BioFlex® culture plates with flexible silicone elastomer bottoms (Flexcell, Hillsborough, NC) coated with 1 mg/ml poly-D-lysine (Sigma). During stretching, computer-programmed vacuum created negative pressure under the BioFlex® culture plates, deforming the flexible membrane in an equibiaxial manner to stretch the cells (Fig. 1*A*) (FX-4000™ Tension System, Flexcell, Hillsborough, NC). The cyclical stretch protocols were designed using the spontaneous contraction amplitude and frequency measured *in vivo* in previous experiments (11). Control cells were subjected to basal cyclical stretch consisting of 0.4-Hz sinusoidal strain with a minimum 1% and a maximum 3% elongation (control cyclical stretch (CCS)), mimicking basal spontaneous contractions. Edema cyclical stretch (ECS) protocol consisted of gradually escalating 0.4-Hz cyclical stretch starting at a minimum 1% and a maximum 3% elongation and reaching a minimum 18% and maximum 20% elongation at 30 min that was maintained for 3.5 h, mimicking the increased stress experienced by smooth muscle cells during edema development. Graphic representation of the two stretching protocols is shown in Fig. 1*B*. Stretched cells were collected at 4 h for further analysis.

Western Blot—After cell stretching or agonist treatment, cells were lysed with whole cell lysis buffer (Cell Signaling, Danvers, MA) with 1× phosphatase inhibitor (Active Motif, Carlsbad, CA) and 1× protease inhibitor mixture (Sigma). After centrifugation, proteins were separated by SDS-PAGE. For the Phos-tag, 12.5% Phos-tag SDS-PAGE with 25 mM Mn^{2+} was prepared as described (33). For all other Western blotting, a 4–15% gradient precast SDS-PAGE (Bio-Rad) or a 4–12% gradient precast SDS-PAGE (Invitrogen) and 15% regular SDS-PAGE were used. Antibodies used were MLC Thr-18/Ser-19 and MLC Ser-19 (Cell Signaling), MLC Thr-18, and total MLC (Santa Cruz Biotechnology, Inc., Santa Cruz, CA), MYPT1 Thr-696 and MYPT1 Thr-850 (Millipore, Billerica, MA), total MYPT1 (BD Biosciences), PAK1 and PAK2 (Cell Signaling), and GAPDH (Santa Cruz Biotechnology, Inc.). ImageJ from the National Institutes of Health (34) was used to quantify luminescence intensities.

For Western blotting of tissues, mucosa was removed immediately after collection of intestine, and smooth muscle tissue was washed with 10% trichloroacetic acid in acetone with 10 mM DTT once and followed with 100% acetone with 10 mM DTT for three times. The tissues were then frozen in liquid nitrogen. After lyophilization, the tissue was ground over liquid nitrogen and then suspended in 200 μl of 1× sample buffer (100 mM DTT, 10% glycerol, 0.01% bromphenol blue, 60 mM Tris-HCl,

2% SDS, pH 6.8), boiled at 95 °C for 5 min. Then the samples were rotated in 4 °C overnight before loaded in SDS-PAGE (35).

PAK Activity Assay—PAK activity in hISMCs was determined by the HTScan® PAK1 kinase assay kit (Cell Signaling), following the protocol provided by manufacturer. Briefly, whole cell lysates were co-incubated with vehicle or 10 μM IPA-3 for 30 min. Lysates were then incubated with biotin-conjugated phosphotyrosine hydroxylase (Ser-40) in reaction buffer provided by the manufacturer for 30 min at room temperature before incubating on a streptavidin-coated plate. After incubating with phosphotyrosine hydroxylase (Ser-40) antibody and HRP-conjugated secondary antibody, absorbance was measured (VersaMax^{TM} plate reader, Molecular Devices, Sunnyvale, CA) at a 450-nm wavelength.

To determine the PAK activity level in intestinal smooth muscle tissues, distal small intestine (ileum) was collected in ice-cold Kreb's solution (119 mM NaCl, 9.6 mM KCl, 15 mM $NaHCO_3$, 1.5 mM $CaCl_2$, 1.2 mM $MgCl_2$, 1.2 mM NaH_2PO_4, 11 mM D-glucose, 0.5% albumin, pH 7.4). After removing the mucosa, samples were quickly frozen and pulverized over liquid nitrogen. Muscle tissue lysates were prepared using the Protein Extract Kit following the manufacturer's protocol (Active Motif). Kinase activity toward MYPT1 was measured by co-incubating tissue lysates with MYPT1 peptide (MYPT1654-880, Cell Signaling) in reaction buffer (25 mM Tris-HCl, 5 mM β-glycerophosphate, 2 mM DTT, 0.1 mM sodium orthovanadate, 10 mM $MgCl_2$, 250 μM ATP) with 2.5 μCi of [γ-^{32}P]ATP. Specific PAK activity toward MYPT1 was determined by pretreating tissue lysates with the PAK-specific inhibitor, IPA-3 (Tocris, Ellisville, MO).

To determine PAK activation with BPIPP treatment, PAK1 (1.25 μg/ml), PAK2 (1.25 μg/ml; ProQuinase (Freiburg, Germany)), or PAK5 (2.5 μg/ml; Abcam (Cambridge, MA)) was pretreated for 10 min with 50 μM BPIPP or 0.1% DMSO and GST-tagged MYPT1(654–880) (25 μg/ml; Millipore) was phosphorylated in reaction buffer containing 40 mM triethanolamine, pH 8.0, 2 mM DTT, 1 mM EDTA, 10 mM $MgCl_2$, and 50 μM ATP with 800,000 cpm/nmol [γ-^{32}P]ATP (PerkinElmer Life Sciences) at 30 °C for 10 min. Reactions were stopped by spotting onto p81 filters. MYPT1 phosphorylation was measured in triplicate and normalized to total protein kinase activity. BPIPP was a generous gift from Scott Gilbertson (Department of Chemistry, University of Houston).

DNA and siRNA Transfection of hISMCs—hISMCs were seeded in 6-well BioFlex® culture plates 1 day before transfection to reach the desired confluence (70%) on the day of transfection. Fugene6 (Roche Applied Science) was used to transfect 2 μg/well DNA plasmids into hISMCs according to the manufacturer's protocol. Briefly, 3 μl of Fugene6 reagent was pipetted into 97 μl of serum-free medium and incubated for 5 min before 2 μg of DNA was added. After incubating for an additional 15 min at room temperature, the medium containing Fugene6 reagent and DNA was added into one well of a 6-well plate. The constitutively active (pCMV6M-hPAK1L107F) and kinase-negative (pCMV6M-hPAK1K299R) PAK1 plasmids were generous gifts from Dr. Jonathan Chernoff (36). Lipofectamine^{TM} RNAiMAX (Invitrogen) was used to transfect 3 pmol/well siRNA into hISMCs following the manufacturer's protocol. Briefly, 3 pmol/well siRNA was added into another 250 μl of serum-free Opti-MEM medium (Invitrogen). At the same time, 3 μl of Lipofectamine^{TM} RNAiMAX was mixed into another 250 μl of serum-free Opti-MEM medium. After incubating for 5 min at room temperature, medium containing siRNA or Lipofectamine^{TM} RNAiMAX was mixed together and incubated at room temperature for 15 min. The mixture was added into one well in a 6-well plate. Fresh medium was added after 4 h, and cells were collected after 48 h. Three predesigned PAK1 siRNAs and three predesigned PAK2 siRNAs were used (Sigma). Two days after transfection, cells were collected for analysis.

Rat Intestinal Edema Model—All procedures were approved by the University of Texas Medical School Institutional Animal Care and Use Committee and are consistent with the National Institutes of Health Guide for the Care and Use of Laboratory Animals. Intestinal edema was induced in male Sprague-Dawley rats weighing between 250 and 350 g as described previously (14). Briefly, intestinal edema was induced by a combination of mesenteric venous hypertension and fluid administration (80 ml/kg, 0.9% NaCl). Control-operated animals underwent laparotomy and gut manipulation but no mesenteric venous hypertension and saline infusion. 6 h after surgery, the animals were sacrificed, and small intestines were collected for contractile function and kinase assays.

Intestinal Tissue Contractile Activity—Intestinal contractile activity, in the longitudinal axis, was measured 6 h after surgery as described previously (14). Isometric force was monitored by an external force displacement transducer (Experimetria Ltd., Budapest, Hungary) connected to a PowerLab (AD Instruments, Colorado Springs, CO). The force displacement transducer was calibrated in grams using a known weight. Each strip was stretched to 0.5-g tension and allowed to equilibrate for 30 min. After equilibration, 10 min of basal contractile activity data were recorded. IPA-3 or vehicle (DMSO) was added to the chamber, and 5 min of additional data were collected. A dose-response curve for IPA-3 was performed to select the optimal dose. After recording contractile activity, the length of each strip was measured, and tissue was removed, dried, and weighed. Contractile activity parameters were all calculated over 5 min of recorded data. Total contractile activity was calculated as area under the curve. Basal tone was defined as the average minimum of the contraction cycle. Amplitude was calculated as average cycle height. All contractile activity parameters were normalized to tissue cross-sectional area of the intestinal strip calculated using measured weight and length and an assumed density of 1.05 g/cm^3.

Statistical Analyses—At least three independent repetitions were conducted for each cell experiment and presented as means ± S.D. Data were analyzed by unpaired Student's *t* tests or analysis of variance to determine significance.

RESULTS

Effect of Mechanical Stretching on MLC Phosphorylation—To study the detailed mechanism of cellular response to mechanical stimulation, a primary hISMC model was developed. hISMCs were isolated and characterized by flow cytometry using the smooth muscle cell markers, smooth muscle actin and desmin, and the endothelium cell marker, CD34. Our

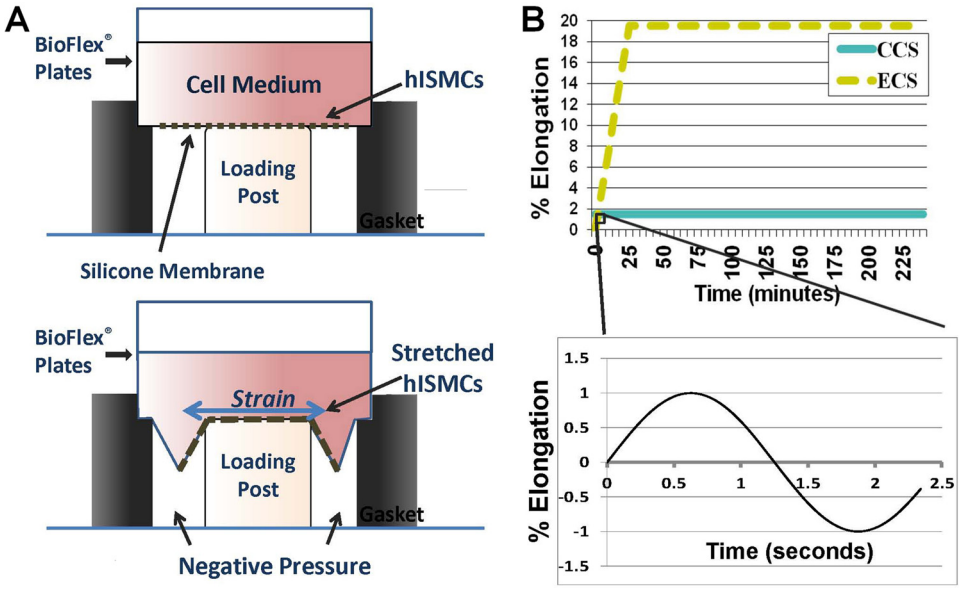

FIGURE 1. **Schematic diagram of hISMCs cyclical stretching model.** *A*, flexible bottom plates were placed on the Flexcell® FX-4000™ tension station. Computer-regulated vacuum applied negative pressure under the flexible bottom to produce equibiaxial cyclic strain to hISMCs cultured on the plate. *B*, *top*, schematic diagram shows ECS and CCS stretching protocols. Each cyclical stretching protocol is a sinusoidal wave with a frequency of 0.4 Hz and an amplitude of 2% elongation over 4 h with no prestretch. The hISMCs in the CCS group were subjected to continual cyclical stretch with a minimum 1%, maximum 3% elongation for the entire 4-h time period. The hISMCs in the ECS group were subjected to a gradually increasing elongation but the same frequency and waveform beginning at minimum 1%, maximum 3% elongation, increasing until reaching minimum 18%, maximum 20% elongation at 30 min, and remaining at this level of cyclical strain for the rest of the time course (3.5 h). *Bottom*, schematic diagram shows cyclical stretching in a 2.5-s time frame. hISMCs in both CCS and ECS groups were subjected to a sinusoid (0.4 Hz, amplitude 2%) radial strain during the whole stretching time course.

hISMCs were compared with commercially available hISMCs (Sciencell, Carlsbad, CA) as a positive control. According to flow cytometry data, 93% of cells from the first passage of hISMCs were positive for both smooth muscle actin (supplemental Fig. 1) and desmin (data not shown). Less than 0.1% of the cells were positive for CD34.

As described under "Experimental Procedures," hISMCs were subjected to either CCS or ECS protocols (Fig. 1*B*), mimicking non-edematous and edematous conditions *in vivo* (11). We first determined the time course of MLC phosphorylation changes after cells were subjected to CCS or ECS. MLC phosphorylation decreased within 2 h of ECS compared with CCS and further decreased after 4 h of ECS (suplemental Fig. 2*A*). MLC was separated into unphosphorylated MLC and monophosphorylated and diphosphorylated MLC using Phos-tag SDS-PAGE (33). Both mono- and diphosphorylation bands were detected (supplemental Fig. 2*B*). Decreases in diphosphorylation bands were observed after 4 h of ECS compared with CCS treatment (supplemental Fig. 2*B*).

Thr-18 and Ser-19 are the two major MLC phosphorylation sites (37, 38). In order to determine the effect of the mechanical stimulation, MLC phosphorylation in the CCS group was compared with MLC phosphorylation in the static cells using antibodies that specifically recognize diphosphorylated MLC (Thr-18 and Ser-19), Ser-19-phosphorylated MLC, and Thr-18-phosphorylated MLC. No significant differences were observed in diphosphorylation and phosphorylation at the Thr-18 site in the CCS group compared with static cells (supplemental Fig. 3, *A* and *C*). However, Ser-19 phosphorylation increased significantly in the CCS group compared with static cells (supplemental Fig. 3*B*).

Similar to the observation in Phos-tag SDS-PAGE experiments, diphosphorylation of MLC after 4 h of ECS treatment was decreased to 65 ± 11% compared with CCS treatment (Fig. 2*A*). Ser-19 phosphorylation of MLC was decreased to 42 ± 12% after 4 h of ECS compared with CCS (Fig. 2*B*). In contrast, Thr-18 phosphorylation was not significantly changed in the ECS group compared with CCS (Fig. 2*C*). These data suggested that Ser-19 phosphorylation, which exists in both diphosphorylated MLC and single Ser-19-phosphorylated MLC, is more sensitive to mechanical stimulation in hISMCs. Thus, it is the major phosphorylation site we monitored in all subsequent studies. Because hISMCs experience continued mechanical stress under physiological conditions similar to CCS treatment, in all subsequent experiments, CCS was the control for ECS treatment.

Effect of Mechanical Stretching on MYPT1 Phosphorylation and PAK Activity—MLC phosphatase is inhibited by phosphorylation of its MYPT1 subunit (18); thus, decreased MYPT1 phosphorylation will increase phosphatase activity. Inhibitory phosphorylation of MYPT1 was monitored after 4 h of ECS or CCS. ECS significantly decreased MYPT1 phosphorylation at both Thr-696 and Thr-853 (Fig. 3, *A* and *B*). These data suggest that MLC phosphatase activity is increased. These data agree with our findings in the *in vivo* intestinal edema model in which intestinal smooth muscle MLC and MYPT1 phosphorylation is decreased (7, 14). Previous studies have indicated that PAK is responsive to mechanical signals and can regulate MLC phosphatase activity (22, 27, 39, 40). PAK activity was measured in hISMCs after stretching (CCS or ECS). A significant increase in kinase activity toward the PAK substrate was observed in the ECS group compared with CCS (Fig. 3*C*). Preincubating the whole cell lysates with 10 μM IPA-3, a group 1 PAK (PAK1 to -3)

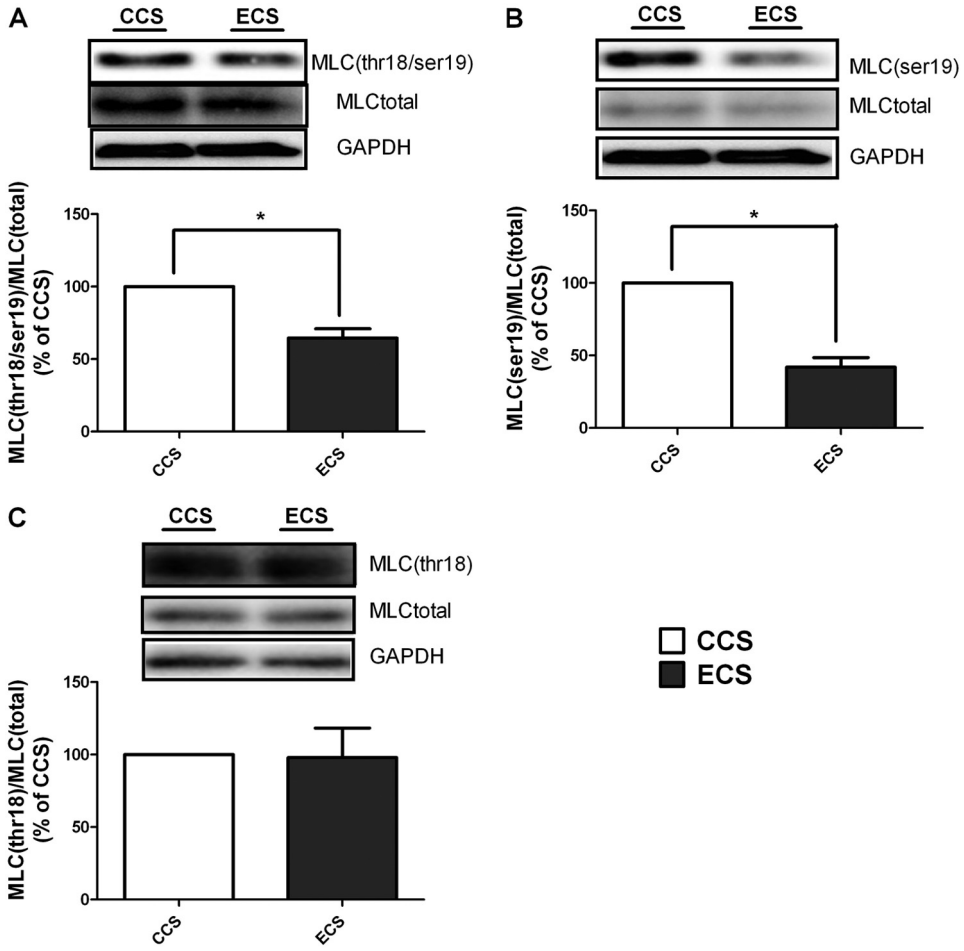

FIGURE 2. **Phosphorylation of MLC is decreased significantly after 4 h of ECS compared with CCS.** MLC diphosphorylation (Thr-18/Ser-19) (*A*), MLC (Ser-19) phosphorylation (*B*), and MLC (Thr-18) phosphorylation (*C*) were monitored by Western blotting. Representative Western blots are shown for each protein as indicated, and the ratio of the phosphorylated protein to the total protein is shown in the *bottom panels*. *, $p < 0.05$ *versus* CCS; $n = 3$/group. *Error bars*, S.D.

inhibitor (34), for 30 min significantly decreased kinase activity toward the PAK substrate in both groups. After IPA-3 treatment, the basal kinase activity was not significantly different between CCS and ECS, suggesting that the increased kinase activity in the ECS group resulted from the PAK activity (Fig. 3*C*).

Effects of IPA-3 and BPIPP Treatment—To determine PAK involvement in regulation of MLC and MYPT1 phosphorylation, IPA-3 (41) and a PAK activator, BPIPP, were utilized. Inhibition of PAK with IPA-3 decreased MLC Ser-19 phosphorylation in hISMCs in a dose-dependent manner in the CCS group (Fig. 4*A*). In contrast, low dose IPA-3 treatment (100 nM) rescued the decreased MLC Ser-19 phosphorylation in the ECS group (Fig. 4*A*). Moreover, IPA-3 regulated MLC Ser-19 phosphorylation in a biphasic manner in the ECS group, first increasing MLC Ser-19 phosphorylation at the 100 nM concentration and then returning to vehicle control levels with application of higher inhibitor concentrations.

Similar to IPA-3, activation of PAK with BPIPP also regulated MLC Ser-19 phosphorylation in a biphasic manner in the CCS group (Fig. 4*B*). Low dose BPIPP treatment increased MLC Ser-19 phosphorylation in CCS; however, high BPIPP concentration decreased MLC Ser-19 phosphorylation. The same phenomenon was observed in static cells, where low concentrations of BPIPP increased but higher concentrations decreased MLC Ser-19 phosphorylation in hISMCs (supplemental Fig. 4*A*). Changes in MLC phosphorylation with BPIPP treatment were confirmed by immunofluorescence (supplemental Fig. 4, *B–D*). In contrast to the CCS group, BPIPP treatment in ECS, in which PAK activity is higher (Fig. 3*C*), decreased MLC phosphorylation at Ser-19 (Fig. 4*B*).

Determining PAK Subtypes Involved in Regulation of MLC Phosphorylation—As shown in Fig. 5*A*, group 1 PAKs (PAK1 to -3), but not group 2 PAKs (PAK4 to -6), are activated by BPIPP and can directly phosphorylate MYPT1 *in vitro*. To determine which group 1 PAK is involved in regulating MLC phosphorylation, PAK1 and PAK2 siRNA were utilized to knock down PAK activity. Both PAK1 and PAK2 siRNA specifically knocked down their corresponding proteins in hISMCs (Fig. 5*B*). Transfection with PAK1 siRNA, but not PAK2 siRNA, significantly down-regulated MLC Ser-19 phosphorylation in static hISMCs (Fig. 5*C*). Furthermore, PAK1 knockdown had opposite effects in the ECS group compared with the CCS group. Although PAK1 knockdown decreased MLC Ser-19 phosphorylation in hISMCs subjected to CCS, PAK1 knockdown attenuated ECS-induced decreases in MLC Ser-19 phosphorylation (Fig. 5*D*).

Effects of Constitutively Active PAK1 (ca-PAK1) or Kinase-negative PAK1 (kn-PAK1) on MLC Phosphorylation— ca-PAK1 and kn-PAK1 were utilized to further investigate the role of

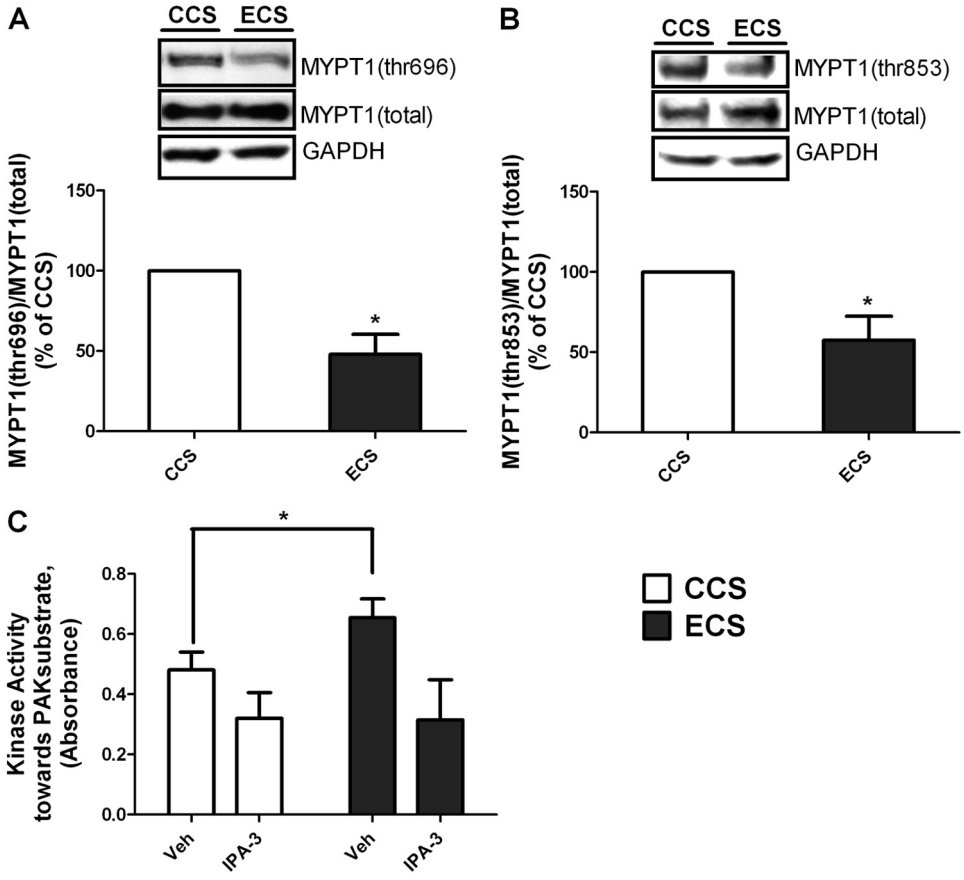

FIGURE 3. **4-h ECS significantly decreased phosphorylation of MYPT1 and increased PAK activity.** MYPT1 (Thr-696) phosphorylation (*A*) and MYPT1 (Thr-853) phosphorylation (*B*) were monitored by Western blotting. Representative Western blots are shown for each protein, as indicated, and the ratio of the phosphorylated protein to the total protein is shown in the *bottom panels*. *, $p < 0.05$ *versus* CCS; $n = 4$/group. *C*, PAK activity increased in the ECS group compared with the CCS group. hISMC lysates from CCS and ECS groups were incubated with vehicle (*Veh*) or IPA-3 (10 μM) for 30 min before kinase activity toward a PAK substrate was measured. *, $p < 0.05$ *versus* vehicle-treated CCS group. $n = 4$/group. *Error bars*, S.D.

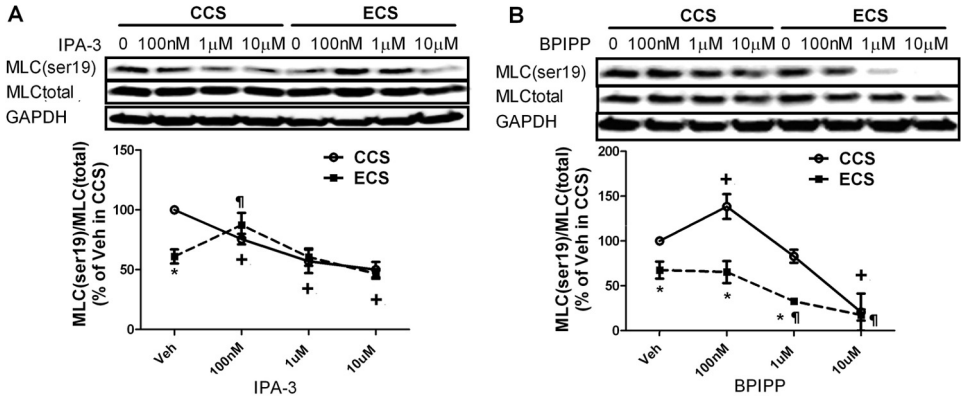

FIGURE 4. **Change of MLC phosphorylation with PAK inhibition or activation.** *A*, change of MLC phosphorylation with IPA-3 treatment in stretched hISMCs. hISMCs were pretreated with varying concentrations of IPA-3 for 30 min before subjecting cells to CCS or ECS. *B*, change of MLC phosphorylation with BPIPP treatment in stretched hISMCs. hISMCs were pretreated with varying concentrations of BPIPP, as indicated, for 30 min before subjecting cells to CCS or ECS. The ratio of phosphorylated to total MLC phosphorylation is shown. *, $p < 0.05$ *versus* CCS group at the same concentrations; +, $p < 0.05$ *versus* vehicle treatment in CCS; ¶, $p < 0.05$ *versus* Veh treatment in ECS; $n = 3$/group. *Error bars*, S.D.

PAK in regulating MLC phosphorylation. PAK1 levels after transfection with ca-PAK1 or kn-PAK1 are shown in Fig. 5*E*. In CCS, transfection with ca-PAK1 increased MLC Ser-19 phosphorylation compared with vector-only transfection. Decreasing PAK1 activity with kn-PAK1 overexpression in CCS inhibited MLC Ser-19 phosphorylation (Fig. 5*E*). In contrast, ca-PAK1 expression did not alter MLC Ser-19 phosphorylation compared with vector-only transfection in ECS, in which PAK activity is already high (Fig. 3*C*). However, kn-PAK1 overexpression attenuated the ECS-induced decrease in MLC Ser-19 phosphorylation. Thus, MLC phosphorylation in the ECS transfected with control plasmid is significantly decreased compared with the CCS group, whereas the ECS transfected with kn-PAK1 is not significantly different from CCS control

(Fig. 5*E*). These data indicate that PAK1 differentially regulates MLC phosphorylation in cells subjected to ECS compared with CCS.

Effects of PAK on MYPT1 Phosphorylation—In our *in vivo* model, MLC phosphorylation was decreased via decreased inhibitory phosphorylation of MYPT1 (14). Thus, the effects of PAK activation on MYPT1 phosphorylation in hISMCs were investigated. Inhibiting PAK1 activity using PAK1 siRNA significantly decreased MYPT1 phosphorylation at Thr-696 in static hISMCs (Fig. 6*A*); however, MYPT1 phosphorylation at

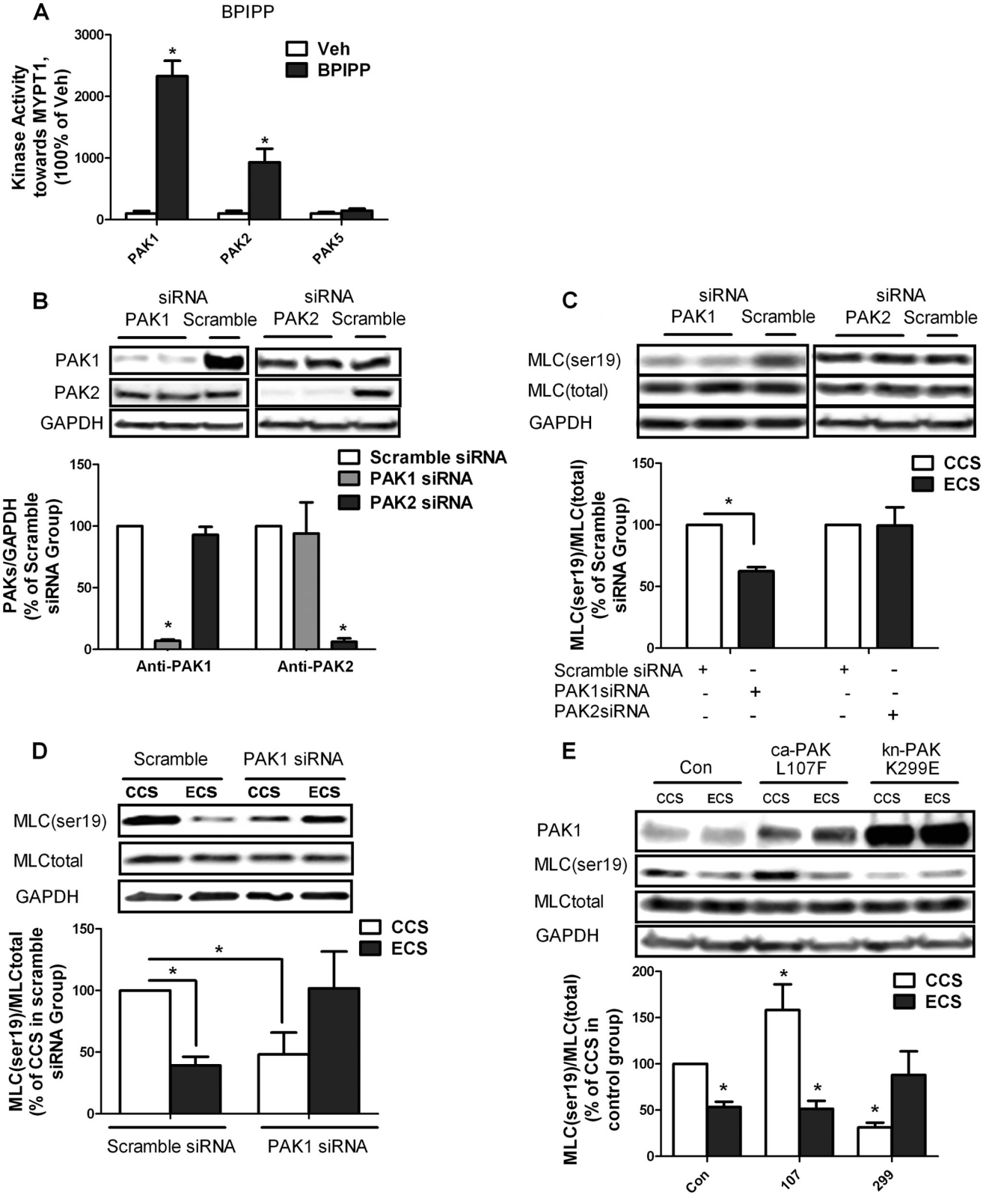

Thr-853 was not affected (Fig. 6*B*). PAK2 siRNA had no effect on MYPT1 phosphorylation in static hISMCs (Fig. 6, *A* and *B*).

Although ca-PAK1 expression tended to increase MYPT1 phosphorylation at Thr-696 in hISMCs subjected to CCS, the differences were not significant. However, decreasing PAK activity with kn-PAK1 significantly decreased MYPT1 phosphorylation at Thr-696 after CCS (Fig. 6*C*). MYPT1 phosphorylation at Thr-696 was significantly decreased in hISMCs subjected to ECS after transfection with vector only compared with CCS group (Fig. 6*C*). Transfection with kn-PAK1 in the ECS group attenuated the decreased MYPT1 phosphorylation at Thr-696 (Fig. 6*C*).

Interestingly, MYPT1 phosphorylation at Thr-853 was significantly decreased in the CCS group after transfection with ca-PAK1; however, transfection with kn-PAK1 had no effect on MYPT1 phosphorylation at Thr-853. MYPT1 phosphorylation at Thr-853 was significantly decreased in hISMCs subjected to ECS compared with CCS after transfection with vector only (Fig. 6*D*). Whereas transfection with ca-PAK1 had little effect on MYPT1 phosphorylation at Thr-853 compared with vector only in the ECS group, transfection with the kn-PAK1 prevented ECS-induced decrease in MYPT1 Thr-853 (Fig. 6*D*).

PAK Involvement in Edema-induced Intestinal Smooth Muscle Contractile Dysfunction—To determine if our findings in the hISMC stretch model extend to an animal model of mechanotransduction, we tested the effects of PAK inhibition in our intestinal edema model. We have shown previously that MLC phosphorylation was significantly decreased in edematous intestinal smooth muscle compared with non-edematous tissue (12–15). As shown in Fig. 7*A*, kinase activity toward MYPT1 also significantly decreased after induction of edema compared with non-edematous control tissue as described previously, suggesting that MLC phosphatase activity was increased. As a result, the MYPT1 phosphorylation at both Thr-696 and Thr-853 significantly decreased *in vivo* (Fig. 7*B*). To determine the involvement of PAKs, tissue lysates were treated with IPA-3 to inhibit PAK activity. Treatment with IPA-3 significantly increased kinase activity toward the MYPT1 substrate in edematous tissue lysates but not non-edematous tissue (Fig. 7*C*). These data indicate that the decreased kinase activity toward MYPT1 phosphorylation in edematous tissue resulted from increased PAK activity in edematous tissue.

To confirm the involvement of PAK in intestinal smooth muscle contractile dysfunction, the effects of PAK inhibition on intestinal contractile activity were measured (Fig. 8*A*). We have previously published that contractile activity, including basal tone and amplitude, is decreased in edematous intestinal smooth muscle compared with non-edematous tissue, as can be observed in Fig. 8*A* (7, 14). Inhibition of PAK with IPA-3 significantly increased the amplitude of intestinal contractions in edematous tissue compared with control (Fig. 8*B*). Basal tone was not significantly different in the edematous tissue after IPA-3 treatment compared with the control tissue ($p = 0.11$) (Fig. 8*D*). These data confirm the critical role of increased PAK activity in mediating contractile dysfunction in edematous tissue.

Fig. 9 shows our hypothetical model for the biphasic effects of PAK on regulation of intestinal smooth muscle MLC phosphorylation. Our current studies demonstrate a novel PAK function in regulating MLC phosphorylation in human smooth muscle. Under physiologic conditions, PAK positively regulates MLC phosphorylation through phosphorylation of MYPT1 at Thr-696. However, under pathologic conditions, overstimulated PAK switches to a different signaling pathway that negatively regulates MLC phosphorylation via decreased MYPT1 phosphorylation at Thr-696 and Thr-853.

DISCUSSION

PAK is an important regulator of mechanotransduction, cell motility, and cytoskeleton formation. Although MLC is one of the most important downstream effectors of PAK, the role of PAK in regulating MLC phosphorylation is still controversial. Our data show that increased PAK activity in stretched intestinal smooth muscle cells negatively regulates MYPT1 phosphorylation and inhibits MLC phosphorylation. MLC phosphorylation strongly correlates with contractility; thus, decreased MLC phosphorylation is likely to result in decreased contractile activity. Along with the *in vivo* studies, these data support the conclusion that edema-induced alterations in PAK activity inhibit intestinal smooth muscle tissue contractile activity. Moreover, using an hISMC model, we further demonstrate that PAKs, especially PAK1, differentially regulate MLC phosphorylation in edematous *versus* non-edematous conditions. This is the first study that shows dual roles for PAK in regulating the downstream effector, MLC, giving us a better understanding of the role of PAK in regulating smooth muscle contraction.

To better understand the functions of PAK in mechanotransduction and the regulation of MLC phosphorylation, a primary hISMC model was utilized. Intestinal smooth muscle cells are not static *in vivo*, and MLC phosphorylation is different for

FIGURE 5. **Determination of PAK subtypes that regulate MLC phosphorylation.** *A*, BPIPP treatment increased MYPT1 phosphorylation through activation of group 1 PAKs. The kinase activity of PAK1, PAK2, and PAK5 toward an MYPT1 peptide was determined with or without 50 μM BPIPP treatment. *, $p < 0.05$ *versus* vehicle (*Veh*); $n = 3$/group. *B*, change of PAK1 or PAK2 protein expression level in static hISMCs after PAK1 or PAK2 siRNA transfection. hISMCs were transfected with 1 nM PAK1, PAK2, or scrambled siRNA for 48 h before collection. PAK1 or PAK2 protein levels were monitored by Western blotting and normalized to GAPDH. The ratio of PAK siRNA to scramble siRNA is shown for each PAK isoform. *, $p < 0.05$ *versus* scramble siRNA-transfected group; $n = 3$/group. *C*, change of MLC phosphorylation in static hISMCs after PAK1 or PAK2 siRNA transfection. hISMCs were transfected with 1 nM PAK1, PAK2, or scrambled siRNA for 48 h before collection for analysis. MLC (Ser-19) phosphorylation was measured by Western blotting and normalized to total MLC amount. The ratio of MLC (Ser-19) phosphorylation after PAK1 or PAK2 siRNA transfection compared with scramble siRNA transfection is shown. *, $p < 0.05$ *versus* scramble siRNA-transfected group; $n = 3$/group). *D*, change of MLC phosphorylation with PAK1 siRNA transfection in CCS or ECS. hISMCs were transfected with 1 nM PAK1 or scramble siRNA for 48 h before cell stretching. MLC (Ser-19) phosphorylation was measured by Western blotting and normalized to GAPDH. The ratio of MLC (Ser-19) phosphorylation after PAK1 siRNA transfection compared with scramble siRNA transfection is shown. *, $p < 0.05$ *versus* scramble siRNA-transfected CCS group; $n = 3$/group. *E*, change of MLC phosphorylation with ca-PAK1(L107F), kn-PAK1(K299E), or CMV6 vector transfection. hISMCs were transfected with 2 μM plasmids 48 h before cell stretching. MLC (Ser-19) phosphorylation was measured by Western blotting and normalized to total MLC. The ratio of MLC (Ser-19) level with ca-PAK1 or kn-PAK1 to vector-only CCS group is shown. *, $p < 0.05$ *versus* control vector-transfected CCS group; $n = 3$/group. *Error bars*, S.D.

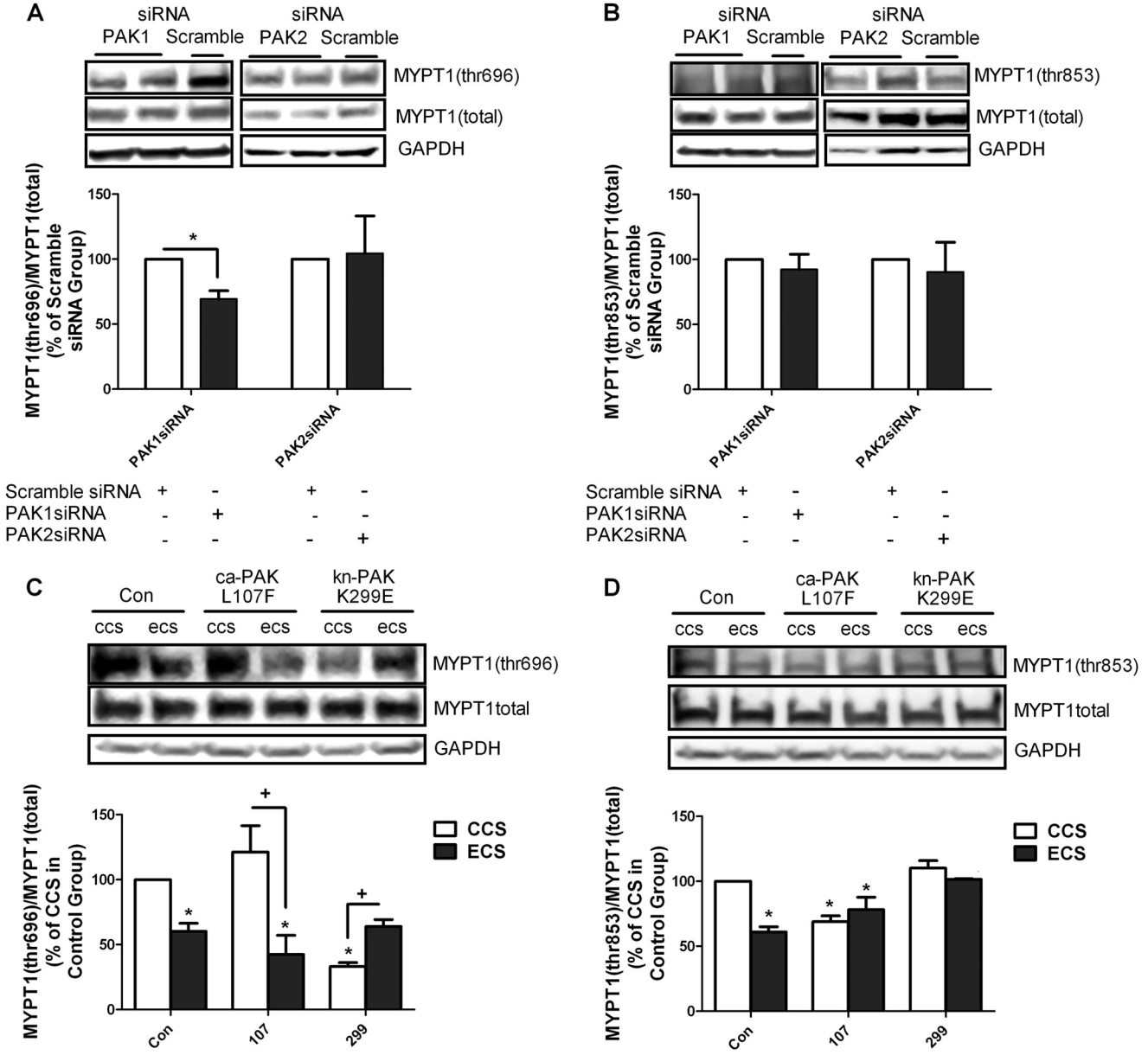

FIGURE 6. **Determination of MYPT1 phosphorylation changes.** Change of MYPT1 (Thr-696) phosphorylation (*A*) or MYPT1 (Thr-853) phosphorylation (*B*) with PAK1 siRNA, PAK2, or scrambled siRNA transfection. hISMCs were transfected with 1 nM PAK1 siRNA or PAK2 siRNA or 1 nM scramble siRNA for 48 h before collection for analysis. MYPT1 (Thr-696) and MYPT1 (Thr-853) phosphorylation were measured by Western blotting and normalized to total MYPT1 amount. Values are shown as a ratio of the scrambled siRNA transfection. *, $p < 0.05$ *versus* scramble siRNA-transfected group; $n = 3$/group. Change of MYPT1 (Thr-696) phosphorylation (*C*) or MYPT1 (Thr-853) phosphorylation (*D*) after transfection with ca-PAK1(L107F), kn-PAK1(K299E), or CMV6 vector. hISMCs were transfected with 2 μM plasmids 48 h before cell stretching. MYPT1 (Thr-696) and MYPT1 (Thr-853) phosphorylation were measured by Western blotting and normalized to total MYPT1. Values are shown as a ratio of the vector-only CCS group. *, $p < 0.05$ *versus* CCS in control vector-transfected group; +, $p < 0.05$ *versus* the indicated CCS group; $n = 3$/group. *Error bars*, S.D.

static cells *versus* contracting cells. Therefore, we designed two stretching protocols to mimic conditions in control (non-edematous) and edematous intestinal smooth muscle, CCS and ECS, respectively. Although diphosphorylation of MLC was not changed after CCS compared with static hISMC, the Ser-19 phosphorylation of MLC was significantly increased in response to the CCS (supplemental Fig. 2). This observation correlates with previous reports that MLC Ser-19 is the primary phosphorylation site for the smooth muscle tissue force generation (16, 17). The increase in Ser-19 phosphorylation in CCS may be due to increased Rac/PAK activity with mechanical stimulation (27, 42) or an activation of MLCK (43). Because hISMCs are usually under mechanical stress *in vivo*, and we showed that CCS affected MLC phosphorylation, we used CCS as the control for ECS.

The stretching protocols utilized in these studies incorporate data from the *in vivo* intestinal edema model, including increased mechanical stress measured during edema development and spontaneous contraction frequency and amplitude measured in the organ bath system (7, 11, 14). Although we have attempted to reproduce the increased stretch that occurs during edema development in intestinal smooth muscle, intestinal edema is a complex phenomenon, and we cannot completely reproduce the effects of edema in a cell model. Further-

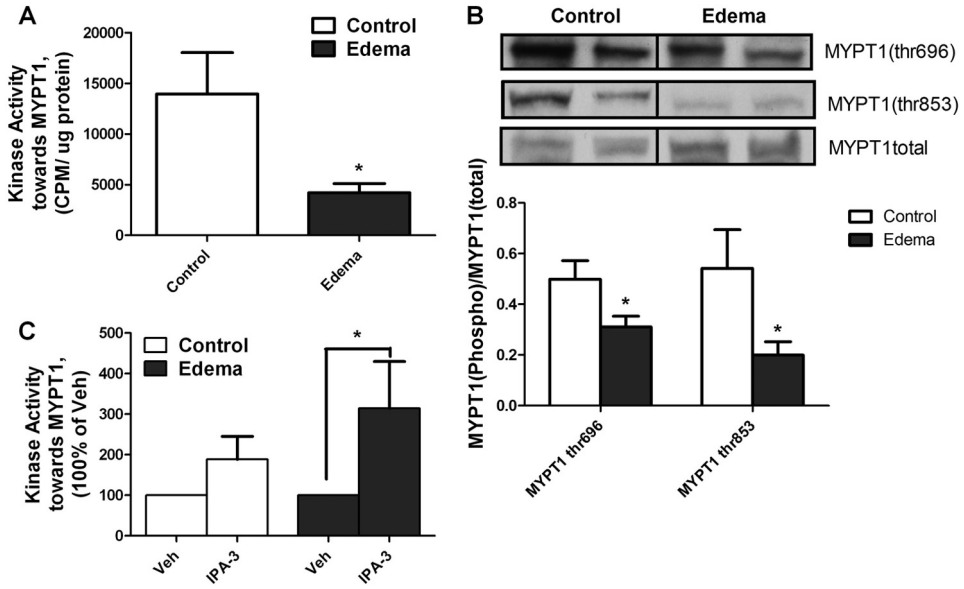

FIGURE 7. **PAK inhibition attenuated the decreased kinase activity toward MYPT1 in edematous tissue.** *A*, kinase activity toward MYPT1 decreases 6 h after edema development. Kinase activity toward MYPT1 peptide in control or edematous intestinal smooth muscle tissues was determined. *, $p < 0.05$ *versus* control; $n = 6$/group. *B*, change of both MYPT1 (Thr-696) phosphorylation and MYPT1 (Thr-853) phosphorylation 6 h after edema development. Rat intestinal smooth muscle tissues from both control and edema groups were isolated and processed as described under "Experimental Procedures." Representative blots are shown along with quantification of the MYPT1 phosphorylation. *, $p < 0.05$ *versus* control; $n = 12$/group. *C*, inhibition of PAK with IPA-3 increased kinase activity toward MYPT1 in edematous tissue. Control or edematous intestinal smooth muscle tissue lysates were pretreated with IPA-3 (10 μM, 30 min) before measuring kinase assay toward an MYPT1 peptide. *, $p < 0.05$ *versus* vehicle (*Veh*); $n = 6$/group. *Error bars*, S.D.

more, although cyclical stretching more closely mimics *in vivo* smooth muscle cells than static cultures, passive stretching does not recapitulate the effects of membrane depolarizations and calcium influx *in vivo*. Thus, this is a mechanotransduction cell model only. Nevertheless, the regulation of MLC phosphorylation in the ECS model parallels observations in edematous intestinal smooth muscle tissue *in vivo* (12–15). Importantly, PAK negatively regulates MLC phosphorylation in hISMCs subjected to ECS just as in the *in vivo* edematous intestinal smooth muscle (Fig. 2). Subjecting cells to ECS significantly increases PAK activity while significantly decreasing both MLC and MYPT1 phosphorylation compared with CCS (7, 14). Thus, subjecting primary hISMCs to ECS is a good model for studying molecular mechanisms by which edema induces decreased MLC phosphorylation. Furthermore, these data suggest that the mechanical changes in intestinal smooth muscle induced by edema may trigger the signaling cascade leading to decreased MLC phosphorylation and eventually decreased intestinal contractile activity. This is supported by the work of Shah *et al.* (15), in which stretching intestinal tissue alone resulted in decreased MLC phosphorylation.

MLC phosphorylation is regulated via both Ca^{2+}-dependent and -independent mechanisms. Ca^{2+}-dependent regulation, involving Ca^{2+}/calmodulin-dependent MLCK, is transient and primarily regulates initiation of smooth muscle contraction (44). In contrast, Ca^{2+}-independent regulation of MLC phosphorylation involves regulation of MLC phosphatase by Ca^{2+}/calmodulin-independent kinases, including ROCK, zipper-interacting protein kinase, and integrin-linked kinase (45, 46). Phosphorylation of the MLC binding subunit of MLC phosphatase, MYPT1, negatively regulates phosphatase activity. Our laboratory has previously demonstrated that edema development in small intestine induces a significant and sustained decrease in intestinal smooth muscle contractile activity via decreased MYPT1 phosphorylation (7, 14). Our current study supports the idea that increased intestinal smooth muscle stretch (edema development) decreases MLC phosphorylation via decreased MYPT1 phosphorylation.

PAK1 has been shown to regulate MLC phosphorylation; however, whether PAK positively or negatively regulates MLC phosphorylation was unclear. An *in vitro* study suggested that PAK can directly phosphorylate MYPT1 at Thr-696, but not Thr-853, to increase MLC phosphorylation (22). PAK activation was also associated with increased MLC phosphorylation in several other studies; however, the involvement of MYPT1 phosphorylation was unclear (30, 31). Negative regulation of MLC phosphorylation by PAKs has also been reported. Several studies have shown that PAK can phosphorylate and inhibit MLCK (28, 29). PAK may also antagonize ROCK, which can phosphorylate MYPT1 to decrease MLC phosphatase activity and, therefore, increase MLC phosphorylation (21, 47). PAK was shown to inhibit ROCK-mediated cytoskeletal rearrangement in several studies (48–50). We present evidence that PAK both positively and negatively regulates MLC phosphorylation, depending on PAK activity level. Moderately increasing PAK activity with the PAK activator, BPIPP, or ca-PAK1 in static hISMCs or hISMCs subjected to CCS resulted in increased MLC phosphorylation. Inhibition of PAK either with IPA-3 or kn-PAK1 inhibited MLC phosphorylation under control conditions. In contrast, in ECS and edematous intestinal smooth muscle, PAK activity is increased and negatively regulates MLC phosphorylation (Figs. 3 and 7). Furthermore, inhibition of PAK in cells subjected to ECS attenuated ECS-induced decreases in MLC phosphorylation, indicating that PAK is negatively regulating MLC phosphorylation under these conditions (Figs. 4*A* and 5*D*). Thus, our study may partially reconcile

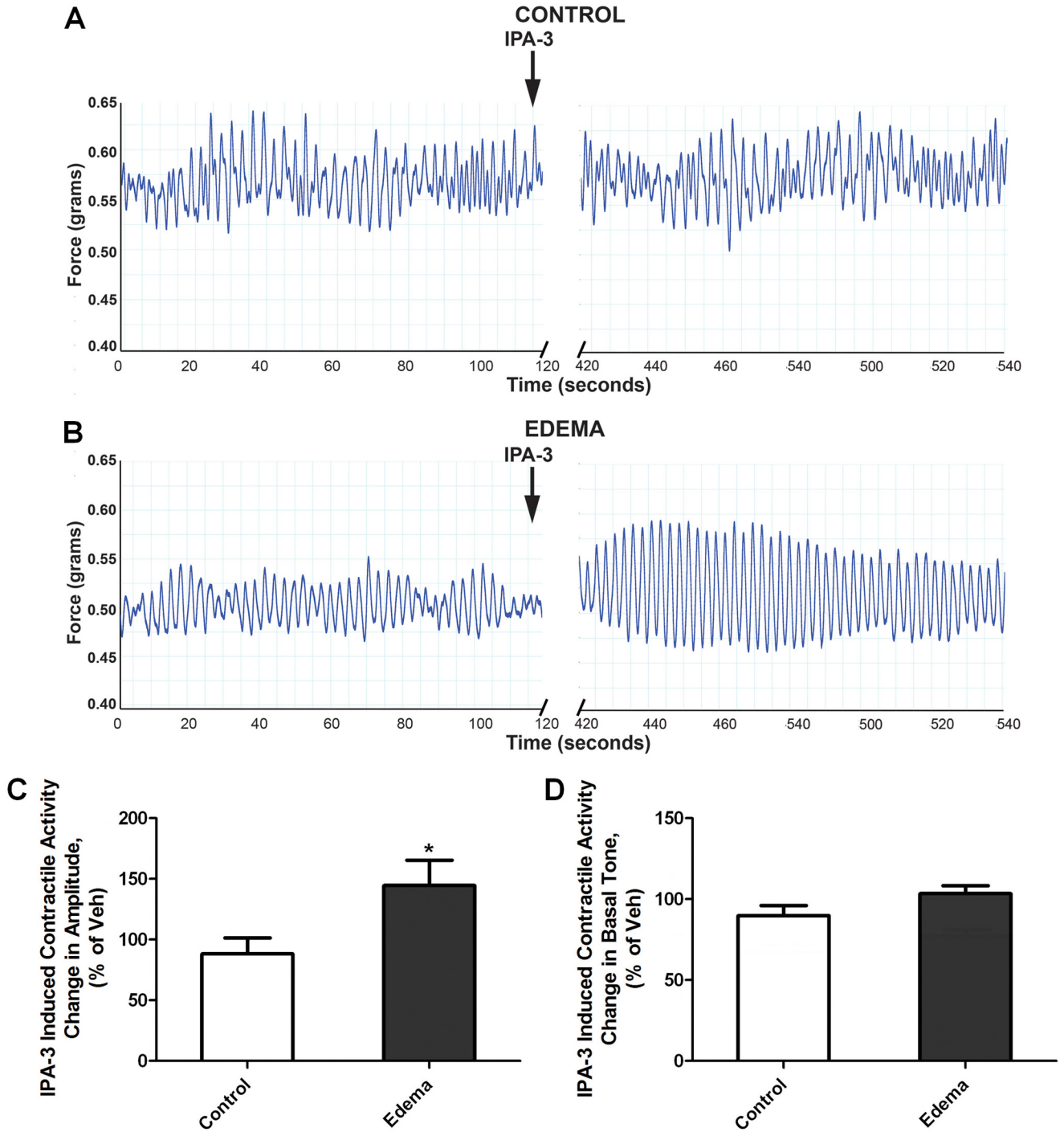

FIGURE 8. **PAK inhibition increased the intestinal smooth muscle contraction in edematous tissues.** Shown are original traces of intestinal tissue spontaneous contractions before and after the addition of IPA-3 (10 μM) in control (*A*) and edema (*B*) groups. Intestinal contractile activity after surgery was monitored in an organ bath. Representative force tracings show the basal intestinal contractile activity before IPA-3 treatment and intestinal contractile activity 5 min after IPA-3 (10 μM) treatment. Effects of PAK inhibition on contraction amplitude (*C*) and basal tone (*D*). Contractile activity was measured 5 min after treatment with vehicle (0.005% DMSO) or IPA-3 (10 μM) in non-edematous (*CONTROL*) and edematous (*EDEMA*) distal small intestine. Data are shown as percentage change from vehicle treatment. *, $p < 0.05$ *versus* control; $n = 8$/group. *Error bars*, S.D.

conflicting reports concerning PAK effects on MLC phosphorylation. PAK inhibition in edematous tissue improved contraction amplitude, suggesting that inhibition of PAK can attenuate edema-induced decreases in intestinal contractility. These data support a critical role of PAK in the regulation of smooth muscle contraction under pathological conditions. IPA-3 treatment did not significantly change the smooth muscle contraction in control tissue. These data combined with the data showing a greater change in kinase activity toward the MYPT1 substrate after IPA-3 treatment in tissue lysates from edematous tissue compared with control (Figs. 7 and 8) suggest that PAK activity is higher in edematous tissue.

PAK-mediated phosphorylation of MYPT1 has been demonstrated *in vitro* (22), but our study is the first to show PAK-

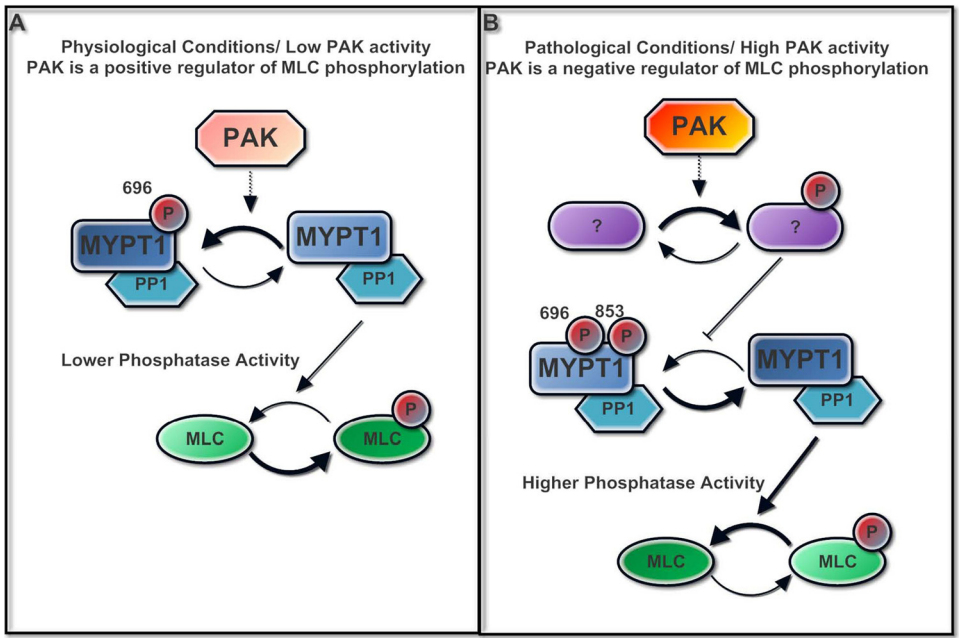

FIGURE 9. **Theoretical model of the dual function of PAK in regulating intestinal smooth muscle myosin light chain phosphorylation.** *A*, under physiologic conditions, PAK positively regulates MLC phosphorylation through phosphorylation of MYPT1 at the Thr-696 site. *B*, under pathologic conditions, overstimulated PAK switches its signaling to a different pathway, which negatively regulates MLC phosphorylation via decreased MYPT1 phosphorylation at both the Thr-696 and Thr-853 sites.

mediated phosphorylation of MYPT1 *in vivo* in smooth muscle cells. Moreover, PAK activation increases MYPT1 phosphorylation at Thr-696, but not Thr-853, in hISMCs subjected to CCS. Knockdown of PAK1 or kn-PAK1 expression decreases phosphorylation at Thr-696 in static or CCS hISMCs (Fig. 6). These data indicate that under physiologic conditions, PAK activation only affects Thr-696. In contrast, subjecting hISMCs to ECS decreases phosphorylation at both Thr-696 and Thr-853. In a previous study, ROCK activity decreased in edematous intestinal smooth muscle tissues (7). ROCK has been shown to phosphorylate MYPT1 at both Thr-696 and Thr-853 (21, 47). Therefore, we speculate that PAK1 positively regulates MLC phosphorylation through phosphorylation of MYPT1 at Thr-696, possibly through direct phosphorylation; however, under pathologic conditions, PAK negatively regulates MLC phosphorylation via inhibition of ROCK-mediated phosphorylation of MYPT1 at both Thr-853 and Thr-696.

We show that increased PAK activity decreases MYPT1 phosphorylation. We speculate that the decreased MYPT1 phosphorylation is due to decreased kinase activity toward MYPT1; however, another possibility is that PAK increases phosphatase activity toward MYPT1. There is some evidence that the catalytic subunit of MLC phosphatase dephosphorylates MYPT1 (51); however, other phosphatases could be involved. Although we give evidence for changes in MLC phosphatase activity, altered MLCK activity is not excluded. There is evidence that PAK can phosphorylate MLCK to inhibit its activity (28, 52). However, in the intestinal edema animal model, no changes in MLCK activity were detected in tissue lysates (7).

The PAK inhibitor, IPA-3, specifically inhibits group I PAKs (PAK1 to -3) (41). Both PAK1 and PAK2 are expressed in intestinal smooth muscle cells, whereas PAK3 is predominantly expressed in neuronal tissue (53) and was not detected in intestinal smooth muscle (data not shown). Previous studies have shown that both PAK1 and PAK2 can regulate MLC phosphorylation (29, 54, 55). We found that siRNA knockdown of PAK1, but not PAK2, inhibits MLC phosphorylation in static cells. Furthermore, PAK1 knockdown in hISMCs prevents ECS-induced decreases in MLC phosphorylation (Fig. 5*D*). PAK1 knockdown also decreased MYPT1 phosphorylation at the Thr-696 site but not the Thr-853 site in static cells. The current study is the first to show a positive regulation of MLC phosphorylation by PAK1 via phosphorylation of MYPT1 at Thr-696 in smooth muscle cells. Although these data suggest a critical role for PAK1 in regulating MLC phosphorylation, the participation of PAK2 cannot be excluded. PAK1 and -2 are highly homologous kinases (53), and regulation of MLC phosphorylation by PAK2 was also reported (54). Interestingly, a recent study has shown that PAK1 and PAK2 have opposing roles in regulating MLC phosphorylation in tumor cells (56).

In conclusion, current studies clearly demonstrate a dual function of PAK in regulating MLC phosphorylation under physiological *versus* pathological conditions. Under physiologic conditions, PAK positively regulates MLC phosphorylation through phosphorylation of MYPT1 at Thr-696. However, increased activation of PAK under pathologic conditions, like edema development, switches PAK signaling to a different pathway involving inhibition of MYPT1 phosphorylation at Thr-696 and Thr-853. The mechanism by which PAK switches from a positive to a negative regulatory role in MLC phosphorylation is unclear. A better understanding of the PAK-mediated MLC phosphorylation regulatory mechanism will help in identifying drug targets for the treatment of motility disorders.

Acknowledgments—We thank Dr. Jonathon Chernoff for generously supplying the constitutively active and kinase-negative PAK1 DNA constructs. We also thank Scott Gilbertson (Department of Chemistry, University of Houston) for the generous gift of BPIPP.

REFERENCES

1. Kasai, Y., Tsutsumi, O., Taketani, Y., Endo, M., and Iino, M. (1995) Stretch-induced enhancement of contractions in uterine smooth muscle of rats. *J. Physiol.* **486,** 373–384
2. Sanders, K. M., and Koh, S. D. (2006) Two-pore-domain potassium channels in smooth muscles. New components of myogenic regulation. *J. Physiol.* **570,** 37–43
3. Farrugia, G., Holm, A. N., Rich, A., Sarr, M. G., Szurszewski, J. H., and Rae, J. L. (1999) A mechanosensitive calcium channel in human intestinal smooth muscle cells. *Gastroenterology* **117,** 900–905
4. Burnstock, G., and Prosser, C. L. (1960) Responses of smooth muscles to quick stretch. Relation of stretch to conduction. *Am. J. Physiol.* **198,** 921–925
5. Mann, J. M., Lam, R. H., Weng, S., Sun, Y., and Fu, J. (2012) A silicone-based stretchable micropost array membrane for monitoring live-cell subcellular cytoskeletal response. *Lab Chip* **12,** 731–740
6. Shi, X. Z., Lin, Y. M., Powell, D. W., and Sarna, S. K. (2011) Pathophysiology of motility dysfunction in bowel obstruction. Role of stretch-induced COX-2. *Am. J. Physiol. Gastrointest. Liver Physiol.* **300,** G99–G108
7. Chu, J., Miller, C. T., Kislitsyna, K., Laine, G. A., Stewart, R. H., Cox, C. S., and Uray, K. S. (2012) Decreased myosin phosphatase target subunit 1 (MYPT1) phosphorylation via attenuated rho kinase and zipper-interacting kinase activities in edematous intestinal smooth muscle. *Neurogastroenterol. Motil.* **24,** 257–2566, e109
8. Kehlet, H., and Holte, K. (2001) Review of postoperative ileus. *Am. J. Surg.* **182,** 3S–10S
9. Balogh, Z., McKinley, B. A., Cocanour, C. S., Kozar, R. A., Valdivia, A., Sailors, R. M., and Moore, F. A. (2003) Supranormal trauma resuscitation causes more cases of abdominal compartment syndrome. *Arch. Surg.* **138,** 637–642; discussion 642–633
10. Norton, J. A., Ott, L. G., McClain, C., Adams, L., Dempsey, R. J., Haack, D., Tibbs, P. A., and Young, A. B. (1988) Intolerance to enteral feeding in the brain-injured patient. *J. Neurosurg.* **68,** 62–66
11. Cox, C. S., Jr., Radhakrishnan, R., Villarrubia, L., Xue, H., Uray, K., Gill, B. S., Stewart, R. H., and Laine, G. A. (2008) Hypertonic saline modulation of intestinal tissue stress and fluid balance. *Shock* **29,** 598–602
12. Uray, K. S., Laine, G. A., Xue, H., Allen, S. J., and Cox, C. S., Jr. (2007) Edema-induced intestinal dysfunction is mediated by STAT3 activation. *Shock* **28,** 239–244
13. Uray, K. S., Wright, Z., Kislitsyna, K., Xue, H., and Cox, C. S., Jr. (2010) Nuclear factor-κB activation by edema inhibits intestinal contractile activity. *Crit. Care Med.* **38,** 861–870
14. Uray, K. S., Laine, G. A., Xue, H., Allen, S. J., and Cox, C. S., Jr. (2006) Intestinal edema decreases intestinal contractile activity via decreased myosin light chain phosphorylation. *Crit. Care Med.* **34,** 2630–2637
15. Shah, S. K., Fogle, L. N., Aroom, K. R., Gill, B. S., Moore-Olufemi, S. D., Jimenez, F., Uray, K. S., Walker, P. A., Stewart, R. H., Laine, G. A., and Cox, C. S., Jr. (2010) Hydrostatic intestinal edema induced signaling pathways. Potential role of mechanical forces. *Surgery* **147,** 772–779
16. Kamm, K. E., and Stull, J. T. (1985) The function of myosin and myosin light chain kinase phosphorylation in smooth muscle. *Annu. Rev. Pharmacol. Toxicol.* **25,** 593–620
17. Somlyo, A. P., and Somlyo, A. V. (1994) Signal transduction and regulation in smooth muscle. *Nature* **372,** 231–236
18. Somlyo, A. P., and Somlyo, A. V. (2003) Ca^{2+} sensitivity of smooth muscle and nonmuscle myosin II. Modulated by G proteins, kinases, and myosin phosphatase. *Physiol. Rev.* **83,** 1325–1358
19. Hirano, K., Derkach, D. N., Hirano, M., Nishimura, J., and Kanaide, H. (2003) Protein kinase network in the regulation of phosphorylation and dephosphorylation of smooth muscle myosin light chain. *Mol. Cell Biochem.* **248,** 105–114
20. Takuwa, Y. (1996) Regulation of vascular smooth muscle contraction. The roles of Ca^{2+}, protein kinase C and myosin light chain phosphatase. *Jpn. Heart J.* **37,** 793–813
21. Ito, M., Nakano, T., Erdodi, F., and Hartshorne, D. J. (2004) Myosin phosphatase. Structure, regulation and function. *Mol. Cell Biochem.* **259,** 197–209
22. Takizawa, N., Koga, Y., and Ikebe, M. (2002) Phosphorylation of CPI17 and myosin binding subunit of type 1 protein phosphatase by p21-activated kinase. *Biochem. Biophys. Res. Commun.* **297,** 773–778
23. Kiss, E., Murányi, A., Csortos, C., Gergely, P., Ito, M., Hartshorne, D. J., and Erdodi, F. (2002) Integrin-linked kinase phosphorylates the myosin phosphatase target subunit at the inhibitory site in platelet cytoskeleton. *Biochem. J.* **365,** 79–87
24. MacDonald, J. A., Borman, M. A., Murányi, A., Somlyo, A. V., Hartshorne, D. J., and Haystead, T. A. (2001) Identification of the endogenous smooth muscle myosin phosphatase-associated kinase. *Proc. Natl. Acad. Sci. U.S.A.* **98,** 2419–2424
25. Katsumi, A., Milanini, J., Kiosses, W. B., del Pozo, M. A., Kaunas, R., Chien, S., Hahn, K. M., and Schwartz, M. A. (2002) Effects of cell tension on the small GTPase Rac. *J. Cell Biol.* **158,** 153–164
26. Dharmawardhane, S., Sanders, L. C., Martin, S. S., Daniels, R. H., and Bokoch, G. M. (1997) Localization of p21-activated kinase 1 (PAK1) to pinocytic vesicles and cortical actin structures in stimulated cells. *J. Cell Biol.* **138,** 1265–1278
27. Zhang, H., Landmann, F., Zahreddine, H., Rodriguez, D., Koch, M., and Labouesse, M. (2011) A tension-induced mechanotransduction pathway promotes epithelial morphogenesis. *Nature* **471,** 99–103
28. Sanders, L. C., Matsumura, F., Bokoch, G. M., and de Lanerolle, P. (1999) Inhibition of myosin light chain kinase by p21-activated kinase. *Science* **283,** 2083–2085
29. Wirth, A., Schroeter, M., Kock-Hauser, C., Manser, E., Chalovich, J. M., De Lanerolle, P., and Pfitzer, G. (2003) Inhibition of contraction and myosin light chain phosphorylation in guinea-pig smooth muscle by p21-activated kinase 1. *J. Physiol.* **549,** 489–500
30. Chew, T. L., Masaracchia, R. A., Goeckeler, Z. M., and Wysolmerski, R. B. (1998) Phosphorylation of non-muscle myosin II regulatory light chain by p21-activated kinase (γ-PAK). *J. Muscle Res. Cell Motil.* **19,** 839–854
31. Ramos, E., Wysolmerski, R. B., and Masaracchia, R. A. (1997) Myosin phosphorylation by human cdc42-dependent S6/H4 kinase/γPAK from placenta and lymphoid cells. *Recept. Signal Transduct.* **7,** 99–110
32. Sells, M. A., Boyd, J. T., and Chernoff, J. (1999) p21-activated kinase 1 (Pak1) regulates cell motility in mammalian fibroblasts. *J. Cell Biol.* **145,** 837–849
33. Hidetaka, K. (2009) Phos-tag Western blotting for detecting stoichiometric protein phosphorylation in cells. *Nat. Protoc.* **2009,** doi: 10.1038/nprot.2009.170
34. Girish, V., and Vijayalakshmi, A. (2004) Affordable image analysis using NIH Image/ImageJ. *Indian J. Cancer* **41,** 47
35. Sutherland, C., and Walsh, M. P. (2012) Myosin regulatory light chain diphosphorylation slows relaxation of arterial smooth muscle. *J. Biol. Chem.* **287,** 24064–24076
36. Sells, M. A., Knaus, U. G., Bagrodia, S., Ambrose, D. M., Bokoch, G. M., and Chernoff, J. (1997) Human p21-activated kinase (Pak1) regulates actin organization in mammalian cells. *Curr. Biol.* **7,** 202–210
37. Ikebe, M., and Hartshorne, D. J. (1985) Phosphorylation of smooth muscle myosin at two distinct sites by myosin light chain kinase. *J. Biol. Chem.* **260,** 10027–10031
38. Ikebe, M., Hartshorne, D. J., and Elzinga, M. (1986) Identification, phosphorylation, and dephosphorylation of a second site for myosin light chain kinase on the 20,000-dalton light chain of smooth muscle myosin. *J. Biol. Chem.* **261,** 36–39
39. Mori, S., Iwaoka, R., Eto, M., and Ohki, S. Y. (2009) Solution structure of the inhibitory phosphorylation domain of myosin phosphatase targeting subunit 1. *Proteins* **77,** 732–735
40. Funk, S. D., Yurdagul, A., Jr., Green, J. M., Jhaveri, K. A., Schwartz, M. A., and Orr, A. W. (2010) Matrix-specific protein kinase A signaling regulates p21-activated kinase activation by flow in endothelial cells. *Circ. Res.* **106,** 1394–1403

41. Deacon, S. W., Beeser, A., Fukui, J. A., Rennefahrt, U. E., Myers, C., Chernoff, J., and Peterson, J. R. (2008) An isoform-selective, small-molecule inhibitor targets the autoregulatory mechanism of p21-activated kinase. *Chem. Biol.* **15,** 322–331
42. Li, C., and Xu, Q. (2000) Mechanical stress-initiated signal transductions in vascular smooth muscle cells. *Cell. Signal.* **12,** 435–445
43. Ding, H. L., Ryder, J. W., Stull, J. T., and Kamm, K. E. (2009) Signaling processes for initiating smooth muscle contraction upon neural stimulation. *J. Biol. Chem.* **284,** 15541–15548
44. Murthy, K. S. (2006) Signaling for contraction and relaxation in smooth muscle of the gut. *Annu. Rev. Physiol.* **68,** 345–374
45. Niiro, N., and Ikebe, M. (2001) Zipper-interacting protein kinase induces Ca^{2+}-free smooth muscle contraction via myosin light chain phosphorylation. *J. Biol. Chem.* **276,** 29567–29574
46. Deng, J. T., Van Lierop, J. E., Sutherland, C., and Walsh, M. P. (2001) Ca^{2+}-independent smooth muscle contraction. A novel function for integrin-linked kinase. *J. Biol. Chem.* **276,** 16365–16373
47. Grassie, M. E., Moffat, L. D., Walsh, M. P., and MacDonald, J. A. (2011) The myosin phosphatase targeting protein (MYPT) family. A regulated mechanism for achieving substrate specificity of the catalytic subunit of protein phosphatase type 1δ. *Arch. Biochem. Biophys.* **510,** 147–159
48. Sheehan, K. A., Ke, Y., and Solaro, R. J. (2007) p21-activated kinase-1 and its role in integrated regulation of cardiac contractility. *Am. J. Physiol. Regul. Integr. Comp. Physiol.* **293,** R963–R973
49. Seasholtz, T. M., Radeff-Huang, J., Sagi, S. A., Matteo, R., Weems, J. M., Cohen, A. S., Feramisco, J. R., and Brown, J. H. (2004) Rho-mediated cytoskeletal rearrangement in response to LPA is functionally antagonized by Rac1 and PIP2. *J. Neurochem.* **91,** 501–512
50. Nimnual, A. S., Taylor, L. J., and Bar-Sagi, D. (2003) Redox-dependent downregulation of Rho by Rac. *Nat. Cell Biol.* **5,** 236–241
51. Kaneko-Kawano, T., Takasu, F., Naoki, H., Sakumura, Y., Ishii, S., Ueba, T., Eiyama, A., Okada, A., Kawano, Y., and Suzuki, K. (2012) Dynamic regulation of myosin light chain phosphorylation by Rho-kinase. *PLoS One* **7,** e39269
52. Murthy, K. S., Zhou, H., Grider, J. R., Brautigan, D. L., Eto, M., and Makhlouf, G. M. (2003) Differential signalling by muscarinic receptors in smooth muscle. m2-mediated inactivation of myosin light chain kinase via G_{i3}, Cdc42/Rac1, and p21-activated kinase 1 pathway, and m3-mediated MLC20 (20 kDa regulatory light chain of myosin II) phosphorylation via Rho-associated kinase/myosin phosphatase targeting subunit 1 and protein kinase C/CPI-17 pathway. *Biochem. J.* **374,** 145–155
53. Bokoch, G. M. (2003) Biology of the p21-activated kinases. *Annu. Rev. Biochem.* **72,** 743–781
54. Zeng, Q., Lagunoff, D., Masaracchia, R., Goeckeler, Z., Côté, G., and Wysolmerski, R. (2000) Endothelial cell retraction is induced by PAK2 monophosphorylation of myosin II. *J. Cell Sci.* **113,** 471–482
55. Rudrabhatla, R. S., Sukumaran, S. K., Bokoch, G. M., and Prasadarao, N. V. (2003) Modulation of myosin light-chain phosphorylation by p21-activated kinase 1 in *Escherichia coli* invasion of human brain microvascular endothelial cells. *Infect. Immun.* **71,** 2787–2797
56. Coniglio, S. J., Zavarella, S., and Symons, M. H. (2008) Pak1 and Pak2 mediate tumor cell invasion through distinct signaling mechanisms. *Mol. Cell Biol.* **28,** 4162–4172